PHYSICAL REVIEW B VOLUME 45, NUMBER 1 1 JANUARY 1992-I

# Optical analog of the permeability of sandstones

B. R. De
*Chevron Oil Field Research Company, P.O. Box 446, La Habra, California 90633-0446*

I. H. H. Zabel and D. Stroud
*Department of Physics, Ohio State University, Columbus, Ohio 43210*

M. A. Nelson
*Chevron Oil Field Research Company, P.O. Box 446, La Habra, California 90633-0446*

(Received 28 May 1991)

We demonstrate a correlation between the transmissivity of sandstones to visible light and their fluid permeability. By means of experiments carried out on sandstone and sand packs, we show that the light transmission increases when the contrast between the indices of refraction of the matrix material and pore-filling fluid is reduced, and that, for a given fluid, it is greatest for rocks with the largest grains. We present qualitative and analytical arguments, and results of a numerical simulation, which account for these correlations. The simulations also yield the space and time distribution of the transmitted light. Finally, we show that light transmission provides a method of mapping the permeability of sandstone without fluid flow, and at high spatial resolutions. Extension of these findings to rocks other than sandstones is discussed.

## I. INTRODUCTION

The nondestructive study of rock interiors employs many types of energy—acoustic, nuclear, x-ray, and microwave—but generally not visible light. Light is not used because it is common experience that visible light cannot penetrate a rock. On the other hand, the individual grains of many consolidated rocks are composed of nonabsorbing material. Thus, if a rock composed of such grains is filled with a pore fluid having a sufficiently similar index of refraction, one expects that light will indeed penetrate such a rock.

In this paper, we present the results of an experimental study of sandstones using visible light. We find not only that light can sometimes be transmitted through sandstone, but also that the transmission coefficient is correlated with an important aspect of the pore structure of the rock—its permeability to fluid flow. In particular, we find that large permeability is correlated with low attenuation of visible light. In view of this correlation, we suggest a new method for mapping the permeability of a porous rock without fluid flow and at a spatial resolution not previously realized.

The permeability $k$ of porous rock is defined by the Darcy relation: $\mathbf{v}=-(k/\eta)\nabla p$, where $\mathbf{v}$ is the fluid velocity, $\eta$ is the fluid viscosity, and $p$ is the hydrostatic pressure. A large permeability is of central importance to the extraction of oil.[1,2] In a rock formation, $k$ typically has considerable spatial variation. In studies of such formations, one is interested in $k$ at many length scales, from millimeters to kilometers. Permeability is usually measured by causing a fluid (typically oil, water, or air) to flow through a portion of rock under the influence of a pressure gradient, the rock sample being contained in a suitable fashion.[3–5] These measurements are laborious and slow, involve boundary conditions that are difficult to interpret,[6] and usually achieve resolutions no finer than a few cm. Attempts have been made to characterize rock permeability on a smaller scale[7–9] and to measure directional permeability in anisotropic rock.[10,11]

Composite media have been extensively studied by optical probes in recent years, especially in the short-wavelength limit.[12–19] Optical probes of permeability may not at first appear to be a suitable alternative to conventional methods, even if light does penetrate a rock. For instance, fluid flow is confined to the pore space, while, if the rock grains and pore fluid are both transparent, light penetrates both rock and pore space. However, rock permeability is strongly affected by typical pore dimensions: fine pores are typically correlated with low permeabilities due to large viscous drag forces created by high surface-to-volume ratios. Similarly, for a given pore fluid, and with grain dimensions $d$ large compared to the wavelength $\lambda$, light will scatter more strongly inside a fine-grained (i.e., fine-pored) rock than in a large-grained one because of the greater number of scattering surfaces. Light is therefore expected to be more strongly attenuated in fine-grained composities. This argument suggests a simple correlation between permeability and light propagation: rocks with low fluid permeability should also tend to attenuate light strongly.

In the next section, we describe light propagation experiments carried out on two types of rocklike composites. In Secs. III and IV, we present a theoretical analysis of these experiments, using both qualitative arguments and numerical calculations to account for the experimental trends. Next, we describe optical experiments on naturally occurring rocks (sandstones) and show that there is

©1992 The American Physical Society

indeed a strong correlation between optical transmission and permeability. We conclude with a demonstration of high-resolution optical mapping of the permeability of a sandstone sample.

## II. EXPERIMENTS ON UNCONSOLIDATED COMPOSITES

To deal with relatively controlled geometries, we have initially studied two types of unconsolidated composites, chosen to resemble natural sandstones: dense packings of spherical glass beads, and packs of rounded, but irregularly shaped, quartz sand grains. Microscopic examination revealed that the glass beads were clear, with smooth spherical surfaces, while the quartz grains were transparent with a slight brownish tinge and multifaceted surfaces[20] that were optically "rough" (i.e. had surface irregularities of a scale much smaller than $d$).[21] The refractive index $n$ of glass is 1.52 at visible wavelengths, while that of quartz is 1.55.[22] Three size-sorted glass bead packs were used. These had size ranges 100–110 $\mu$m (reported as $d=105$ $\mu$m), 170–180 $\mu$m (175 $\mu$m), and 250–300 $\mu$m (275 $\mu$m). Four sand packs were used, with size ranges 53–74 $\mu$m (64 $\mu$m), 74–105 $\mu$m (90 $\mu$m), 88–125 $\mu$m (107 $\mu$m), and 177–250 $\mu$m (214 $\mu$m). The word "size" for the glass beads refers to the diameter of the spherical beads. For the sand grains, the sizes quoted here are defined by the mesh sizes of the sieves used to generate the various batches of sand.

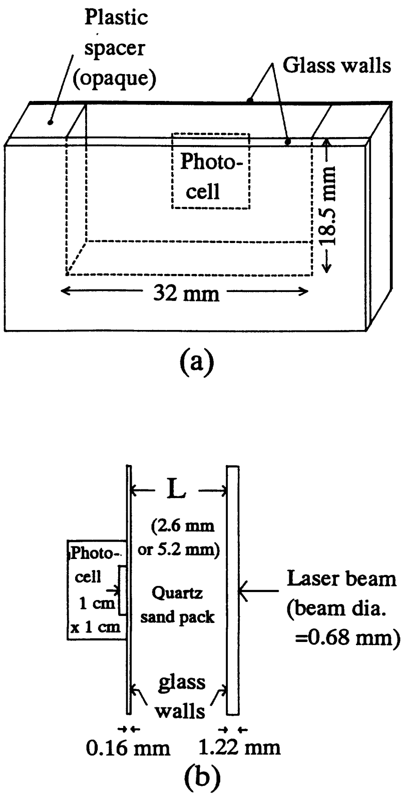

FIG. 1. Experimental setup: (a) sample compartment and (b) measurement geometry.

The glass bead or sand pack was contained in a compartment with glass walls. A 10-mw He-Ne laser was used as a light source (red light, wavelength 632.8 nm, randomly polarized; beam diameter 0.68 mm). The transmitted optical power was measured by a photodetector calibrated for the 632.8-nm wavelength. The area of

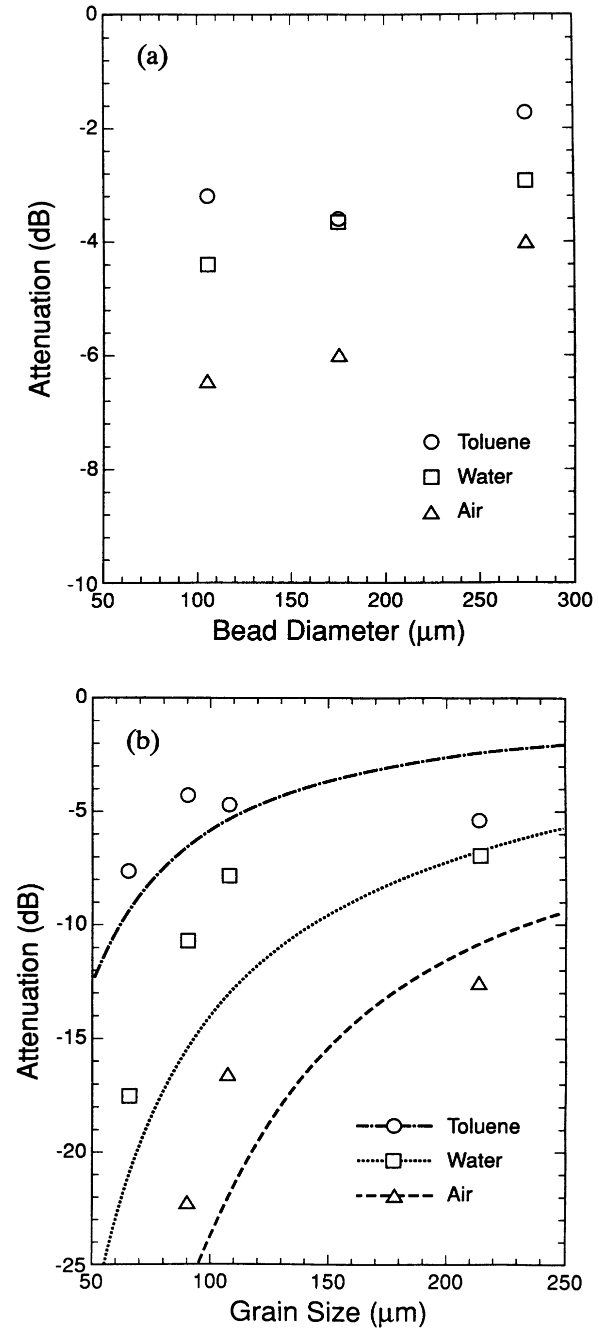

FIG. 2. Optical attenuation of a laser beam of wavelength 632.8 nm through a slab of thickness 2.6 mm of glass bead pack of spherical beads (a) and of sand grain packs comprised of rounded quartz grains (b). Results are shown for several sizes of glass beads or quartz grains saturated with three fluids: (i) air, (ii) water, and (iii) toluene. Continuous curves are the results of numerical simulations.

the photocell, placed flush against the glass wall of the sample compartment, was approximately $1\times 1$ cm$^2$ (Fig. 1). To eliminate the effects of reflection at various interfaces, two sample thickness $L$ (2.6 and 5.2 mm) were studied. The ratio of the two levels $P_1$ and $P_2$ of transmitted power, expressed in decibels, is reported as the attenuation $A$, i.e.,

$$A = 10.0\log_{10}(P_2/P_1)\ \text{dB}\ . \tag{1}$$

The attenuation includes both the loss due to beam scattering, as well as any actual absorption in the constituents. In our samples, however, the measured loss is almost entirely due to the former cause: true absorption is very small.

Measurements were carried out on packs saturated with three fluids: (i) air, (ii) brine with a resistivity of 0.2 $\Omega$ m, and (iii) a fluid consisting of 93% toluene and 7% paraffins of refractive index similar to toluene. In case (ii), a separate experiment showed that the results of the optical experiment were the same with either brine or distilled water. The various saturating fluids have indices of refraction $n_{\text{air}} = 1.00$, $n_{\text{water}} = 1.33$, and $n_{\text{toluene}} = 1.49$.[22]

The results of the attenuation measurements are presented in Fig. 2. The experimental uncertainty of the measurements is estimated to be less than 1 dB. These results suggest three main conclusions: (i) the attenuation is dependent on the size parameter $d$ of the beads or grains, smaller sizes being correlated with larger attenuation, (ii) the attenuation, for a given $d$, decreases as the refractive indices of the matrix and pore fluid become more similar, and (iii) for a given $d$, and given pore fluid, the attenuation is generally much larger for the quartz grains than for the glass beads.

In order to have an independent estimate of the porosities of the sand and bead packs, the dc resistivity of each brine-saturated bead and sand pack was measured under identical conditions. These resistivities were found to be nearly equal for all the glass or sand packs considered, suggesting that the porosities $\phi$ (volume fraction occupied by pore space) were also approximately equal. Thus, not surprisingly, the results of Fig. 2 cannot be explained as a dependence of transmission on porosity.

## III. QUALITATIVE THEORETICAL ARGUMENTS

We now present a simple mean-free-path argument that qualitatively accounts for the general features (i)–(iii) listed above. The transmission coefficient $T$ through a slab (defined as the transmitted power divided by the incident power) depends on, among other parameters, the slab thickness $L$, the indices of refraction $n_1$ and $n_2$ of the rock matrix and the pore fluid, the typical linear dimensions $d$ of the pore or rock grain, and the wavelength $\lambda$ of the incident electromagnetic wave in free space.

To develop a qualitative estimate of the attenuation, we assume that we are in the short-wavelength limit $\lambda \ll d$, which is appropriate for the packs and the frequency considered here. We also assume that the pores have surfaces that are flat on a scale of $\lambda$. A ray traveling through this medium will, on average, encounter a pore/grain interface approximately every distance $d$, being refracted according to Snell's law: $n_1\sin\theta_1 = n_2\sin\theta_2$, where $\theta_1$ and $\theta_2$ are the angles made by the ray in medium 1 and in medium 2 with the surface normal. The justification for considering only the refracted ray is given in Sec. IV. Writing $\theta_2 = \theta_1 + \Delta\theta$, and expanding Snell's law to first order in $\Delta\theta$, we obtain

$$\Delta\theta \approx (n_1 - n_2)\tan\theta_1/n_{\text{av}}\ ,$$

which is valid to first order in $\Delta n/n_{\text{av}}$, where $\Delta n = n_1 - n_2$, and $n_{\text{av}}$ is the volume-averaged index of refraction. The quality $n_{\text{av}}$ here could equally well be taken as $n_1$ or $n_2$ to the same order in $\Delta n/n_{\text{av}}$.

We now use this formula to obtain an estimate of the number of scatterings required before a given ray has lost the memory of its original direction—that is, has been scattered through an angle $\approx \pi/2$ rad. Since $\theta_1$ is a random number depending on the (random) orientation of the surface to the incoming ray, $\tan\theta_1$ is also a random number, of order unity. Thus, to first order in $\Delta n/n_{\text{av}}$, each scattering produces a *change* of angle of order $\Delta\theta \approx \Delta n/n_{\text{av}}$. Since the scattering angle is equally likely to be positive or negative, the root-mean-square change of angle $(\Delta\theta)_N$ produced after $N$ scatterings will be given by a random-walk-like formula, i.e., $(\Delta\theta)_N \approx \Delta n\sqrt{N}/n_{\text{av}}$. The rms number of scattering events $N_c$ required to scatter a given ray through an angle $\pi/2$ will be of order $N_c = [n_{\text{av}}\pi(2\Delta n)^{-1}]^2$. Hence, the "elastic photon mean free path" $l_{\text{el}}$, defined as the distance a photon (i.e., a light ray) will travel before it is scattered through an angle $\pi/2$, is approximately

$$l_{\text{el}} \approx d\left[\frac{n_{\text{av}}\pi}{2\Delta n}\right]^2 . \tag{2}$$

The experimental results (i) and (ii) summarized in the preceding section can be qualitatively understood from this relation. It states that $l_{\text{el}}$ (a) increases with pore or grain size, and (b) increases with decreasing $|\Delta n|$. Since the transmission $T$ through the slab increases with increasing $l_{\text{el}}$, it follows that, for a fixed slab thickness, $T$ should increase with increasing pore size and with decreasing $|\Delta n|$.

Our understanding of the experimental result (iii) is somewhat more speculative. The glass bead pack consists of beads of uniform size and shape, with no surface roughness such as characterizes the sand grains. In applying relation (2) for $l_{\text{el}}$ to grains with rough surfaces, the grain diameter $d$ should more appropriately be replaced by the correlation length $\xi$ characterizing the surface roughness of the grain—that is, the typical distance a photon must travel, on average, before encountering a pore-grain interface. It is shown in the Appendix that a better estimate for $l_{\text{el}}$ is

$$l_{\text{el}} = \frac{4\epsilon_0^2}{\langle(\delta\epsilon)^2\rangle}\frac{\xi}{\ln(2k^2\xi^2)}\ , \tag{3}$$

where $k = 2\pi\sqrt{\epsilon_{\text{av}}}/\lambda$ is the wave number, and $\delta\epsilon$ is the difference between the dielectric constants of the two constituents. Thus, except for logarithmic corrections, $l_{el}$ increases linearly with the correlation length $\xi$. For the glass bead packs, $\xi$ is probably of the order of the bead diameter, or larger, since the surfaces of the beads are smooth. On the other hand, for the quartz grains, $\xi$ is probably smaller than the grain diameter because of variations in grain shape and surface roughness. Hence, this simple formula suggests that, for glass beads and quartz grains of the same nominal diameters, the transmission through the quartz packs should be smaller, as is observed.

## IV. NUMERICAL SIMULATION

We next consider a simulation of propagation in the geometrical optics limit ($\lambda \ll d$), with zero absorption, through a slab of thickness $L$ and infinite extent in the two transverse directions. A ray enters the sample at normal incidence, and propagates a random distance $x$, at which point it is assumed to encounter a pore-grain interface (represented as a randomly oriented planar surface). We follow either the refracted or the reflected ray with probability $R$ or $1-R$, where $R$ is the power reflection coefficient, computed by averaging over polarizations perpendicular and parallel to the plane of incidence:

$$R=\tfrac{1}{2}(|r_{\parallel}|^2+|r_{\perp}|^2) , \tag{4}$$

$r_{\parallel}$ and $r_{\perp}$ being the usual Fresnel amplitudes for reflection of a ray polarized parallel and perpendicular to the surface.[23] Since usually $R \ll 1$, we generally follow the refracted ray.

After scattering from one surface, the randomly chosen (reflected or refracted) ray travels another random distance and meets another randomly oriented surface. The reflected or refracted ray from this surface is again selected at random as described above, and the process continues until the ray exits from the front or the back of the sample. If it reaches the detector, it is counted and its energy, location, and time of arrival are noted. Each ray begins with an energy $\mathcal{E}$ normalized to unity, which is reduced upon each scattering by a factor of $R$ for a reflected ray or $1-R$ for a refracted ray. The transmission coefficient $T$ is calculated as

$$T=f\mathcal{E}_{av} , \tag{5}$$

where $f$ is the fraction of followed rays that reach the detector, and $\mathcal{E}_{av}$ is the average energy of a ray that does reach the detector.[24]

Figure 2(b) shows our results for a sample of quartz grains saturated with three different fluids corresponding to those in the experiment. In each case, the average distance $x_{grain}$ traveled by a ray within a grain between scatterings is taken as $1.5d$, where $d$ is the typical grain size defined in Sec. II. We choose a value slightly larger than $d$, since a ray can travel from one grain to another without passing through the intervening pore space, i.e., by passing through a grain-grain contact area. The distance between scatterings is taken as a random variable uniformly distributed between 0 and $3d$. We choose the typical distance $x_{pore}$ traveled in pore space to be $0.69\times1.5d$, uniformly distributed between 0 and $1.38\times1.5d$. We take $x_{pore}<x_{grain}$ because the estimated porosity $\phi$ of the experimental samples is less than 0.5, so that rays typically travel smaller distances in the pore space. The factor of 0.69 is obtained from the assumption that $\phi=0.25$, which gives

$$x_{pore}/x_{grain}\approx[\phi/(1-\phi)]^{1/3}\approx0.69 .$$

We typically consider $10^5$ rays, which is sufficient to ensure the convergence of $T$ to within a few percent. We deduce the attenuation, as in the measurements, by calculating the transmissions $T_1$ and $T_2$ through two slabs of thickness 2.6 and 5.2 mm. The calculated value of $10\log_{10}(T_2/T_1)$ is quoted as the attenuation (in dB).[25]

The results of the simulation show reasonable agreement with the data for quartz sands over the entire range of grain sizes and for the three types of pore fluids. In particular, the simulation correctly reproduces the increase in attenuation with decreasing grain size, and with increasing contrast between the indices of refraction of pore fluid and grains.

Figure 3 shows the calculated spatial distributions of the transmitted light for quartz saturated with water for several particle sizes. In each case, we have plotted $I(r)$, defined as the transmitted intensity at $z=L=2.6$ mm and at a radial distance $r$ from the axis of the laser beam, given an incident beam normally incident on the slab at $r=0$, $z=0$ of a cylindrical coordinate system. The figure is normalized so that $\int I(r)(2\pi r)dr$ is proportional to the

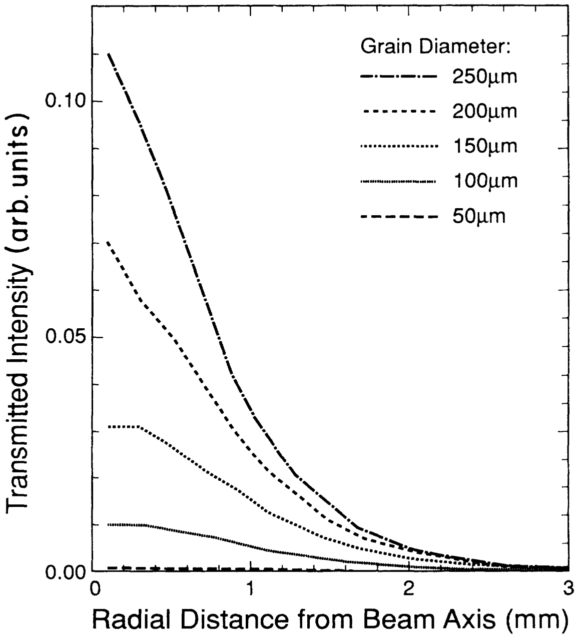

FIG. 3. Calculated transmitted intensity $I(r)$ for 2.6-mm-thick quartz sandpacks of various average grain diameters saturated with water, plotted as a function of the radial distance $r$ from the center of the detector (beam axis). The various intensities are normalized so that for a given particle size, the areal integral $\int I(r)2\pi r\, dr$ equals the transmission coefficient $T$.

total transmission coefficient $T$ for each grain diameter. The half width of the distribution is broadest for the smallest particles, where the rays have been most strongly scattered before emerging from the slab. We have obtained similar graphs for the spatial intensity distributions for quartz saturated with other fluids: in general, for a given slab thickness and particle size, we find, as expected, the spatial distribution is widest when there is the greatest contrast between the indices of refraction of quartz and saturating fluid.

In Fig. 4 we plot the distribution of travel times of the rays for a slab of thickness 2.6 mm containing quartz grains of various sizes and saturated with three different fluids. The figure plots $P(\tau)$, the transmitted power (integrated over the plane $z=L$) at time $\tau$ after the laser beam is incident at the front of the slab, normalized so

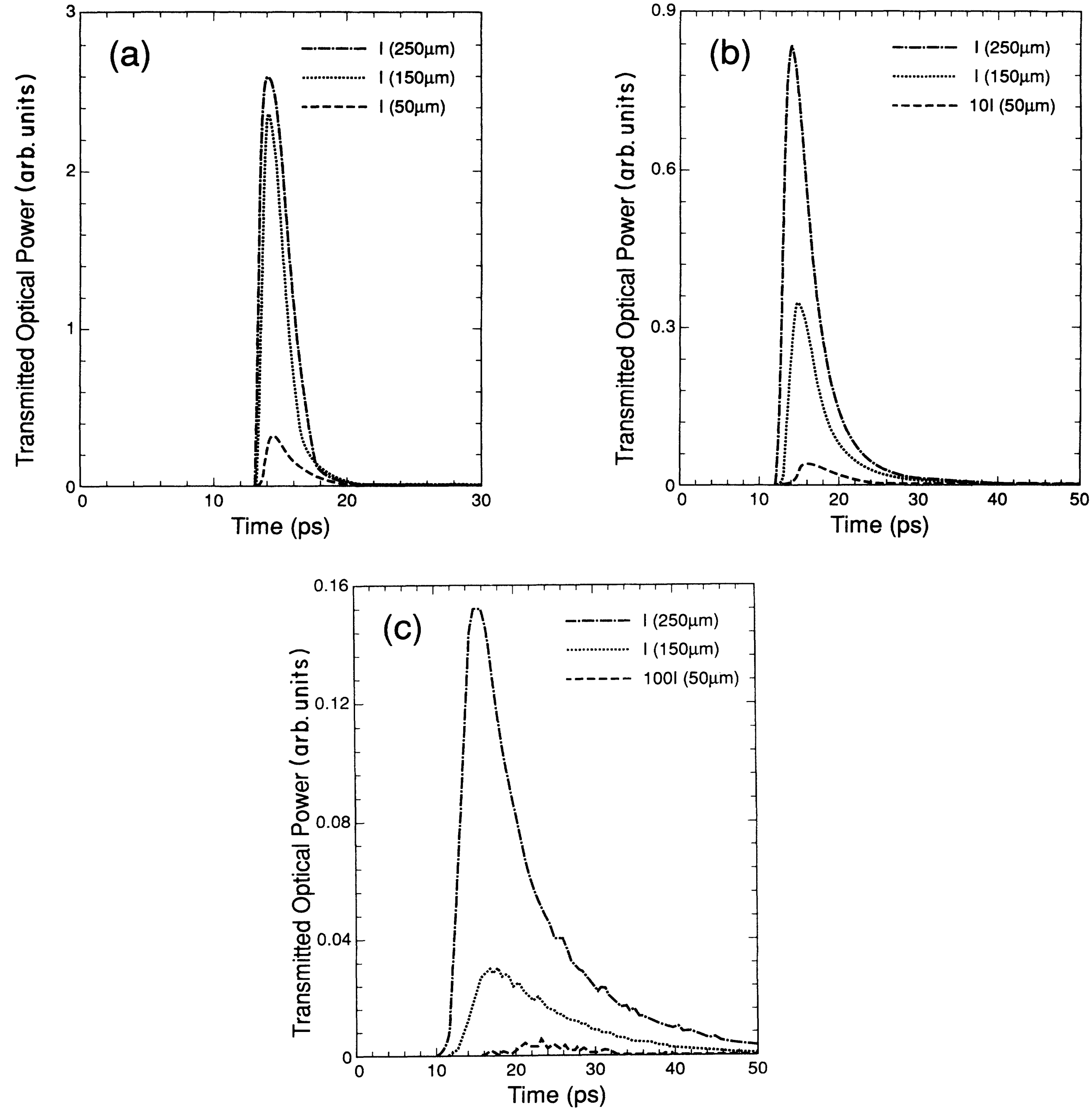

FIG. 4. Calculated transmitted power $P(\tau)$ plotted as a function of arrival time $\tau$, integrated over the surface at $z=L$, for quartz sandpacks of various average particle sizes saturated with toluene (a), water (b), and air (c). Normalization is such that for each saturating fluid, the area under a curve equals the transmission coefficient $T$. The absolute normalization is arbitrary but is the same for each of the three sets of curves.

that $\int P(\tau)d\tau = T$, the transmission coefficient. If the transmission were ballistic, $P(\tau)$ would be a $\delta$ function at $\tau = L/(c/n_{\mathrm{av}})$, where $c/n_{\mathrm{av}}$ is the speed of light in the medium. The width of the distribution once again is seen to increase with increasing scattering within the slab, i.e., with decreasing grain size or increasing index-of-refraction contrast.[26]

The temporal and spatial distributions of arriving pulses suggest other ways of analyzing the transmission through the slab, which may, like the transmission itself, yield information about the permeability, grain size, pore fluid, and other geometrical properties of the medium. Thus an experimental arrangement that could measure these distributions might be of interest in analyzing such properties of the composite.

## V. APPLICATION TO NATURALLY OCCURRING ROCKS

As shown in the previous sections, for a given saturating fluid, the transmission is typically largest for quartz sand packs with the largest grains—the same materials for which the fluid permeability is expected to be largest. Figure 5(a) shows that this expected correlation is also observed in Boise sandstone, a relatively clean (clay-free) sandstone in which the spatial variation of fluid permeability arises from a spatial variation in grain size. The air permeabilities were measured on inch-long, inch-diameter cylindrical plugs, from which 0.2-in.-thick disks were cut. This thickness is small enough to permit a measurable optical transmission through the sample, while at the same time being sufficiently large to be characterized by the permeability of the parent plug. Figure 5(a) displays the measured optical power transmitted through water-saturated samples, plotted against the measured permeability of the samples with respect to the flow of air. There is a clear correlation—large permeabilities correspond to large optical transmissivities. Figure 5(b) shows the optical transmission plotted as a function of the sample porosity, showing that these quantities are uncorrelated.

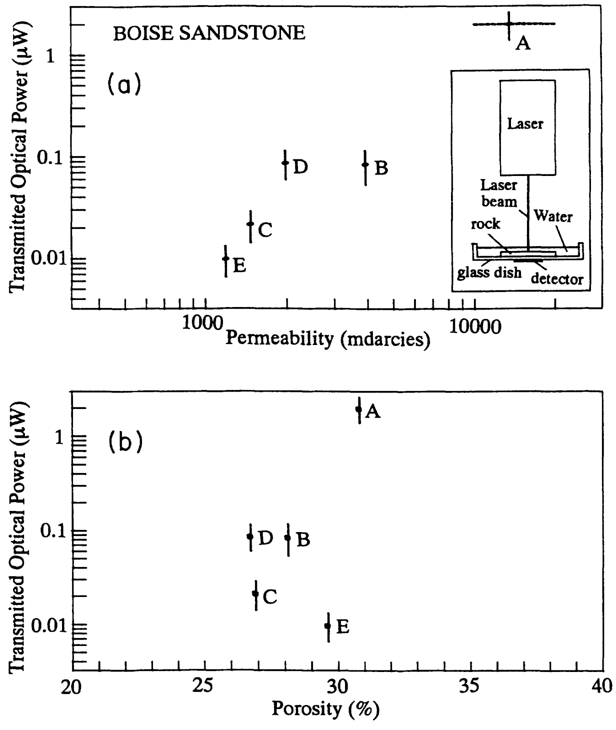

FIG. 5. (a) Transmitted optical power plotted against permeability for five samples of Boise sandstone. Experimental arrangement is shown in the inset. The sample disks, 5 mm thick, are saturated with water and kept immersed in water up to a level 2 mm above the upper surfaces of the samples. The departure from a monotonic correlation exhibited by point B is believed to be due to deviations in thickness from its nominal value. (b) Transmitted optical power plotted against porosity, for the same samples as in Fig. 5(a). No correlation is observed.

Given a theory connecting fluid permeability to light transmission, or a calibration diagram such as Fig. 5(a) for a given type of rock, we can hope to substitute, for some purposes, the optical measurement for the direct measurement of the permeability. The optical measurement can be made with high spatial resolution. Since the laser beam spreads out into an approximately conical volume as it propagates through the sample, this resolution is thickness dependent, the best resolution being obtained for thin samples.

To illustrate the potential use of this method, we have examined a slab of Berea sandstone 10.2 cm square and initially 2.54 cm thick. The sample is homogeneous on large scale but has a stratified structure on a centimeter to millimeter scale with the layers perpendicular to the slab. These layers differ in grain size. A conventional permeability map for the slab was first obtained using a standard air minipermeameter.[9] The measurements were made on grids 1.27 cm square and have a resolution of about 2 cm.

The slab was then sliced down to a thickness of 5.1 mm so as to permit appreciable laser transmission upon saturation with water, while still remaining thick enough to retain bulk permeability characteristics as measured by the minipermeameter. The same face of the slab was presented to the laser beam as to the minipermeameter nozzle. The optical image is shown in Fig. 6(a), taken on grids 1.27 mm square. The experimental arrangement is similar to that shown in the inset of Fig. 5(a), with the sample translated by micrometer stages to obtain areal coverage. The layering is clearly evident. Using a calibration diagram such as Fig. 5(a), one could, in principle, convert the optical transmission to permeability values. This suggests a means of utilizing the optical method to develop an automated permeability mapping system.

In Fig. 6(b) we show the data of Fig. 6(a) replotted after calculating the harmonic mean over every 100 grid squares so that the new grids correspond to those of the miniperimeter measurements. (Arithmetic and geometric means produce similar diagrams.) Data for the perimeter grid points are omitted to avoid anomalous values due to edge effects. Figure 6(c) is the permeability map obtained using the minipermeameter. Within the uncertainties of the measurements, the resemblance between Figs. 6(b)

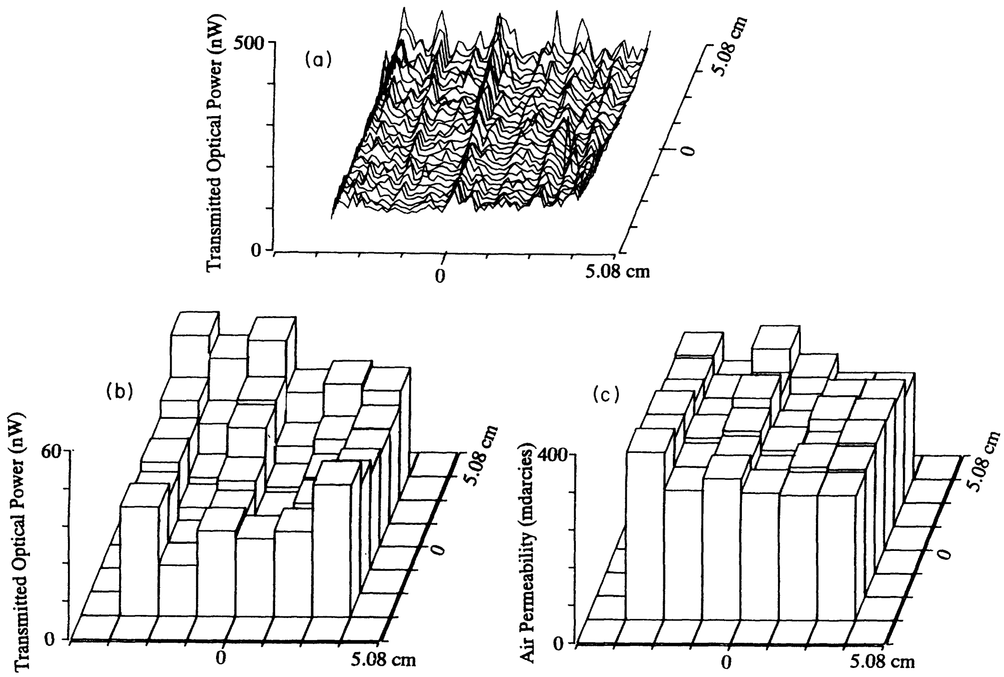

FIG. 6. (a) Optical transmission map of a slab of Berea sandstone. (b) Data of (a) replotted upon averaging over every 100 grid squares. (c) Permeability map for the same slab obtained using an air minipermeameter.

and 6(c) is satisfactory; in particular, the presence of the layers is evident in both sets of measurements. This example suggests how optical and conventional permeability measurements can be combined to test schemes for analyzing the permeability of porous rocks at various length scales.

The same method could be applied, in principle, to other types of rock, such as the carbonates, comprised of limestones and dolomites. In such rocks, unlike clean sandstones, the grains are opaque. Any transmitted light is therefore largely confined to the pore space. Thus we still expect a grain-size-dependent transmission, but probably not a strong dependence of transmission on the refractive index of the pore fluid. Our preliminary experimental studies show that a detectable optical transmission still occurs through limestone, though the attenuation is much greater than in sandstone. The carbonate rocks are therefore best studied using more sensitive detectors or higher-power lasers. Such rocks may exhibit an even stronger correlation between fluid permeability and light transmission than the sandstones, since in the carbonates, both fluid and light flow are confined to the pore space.

## VI. CONCLUDING REMARKS

We have shown that a correlation exists between optical transmission through artificial composites and natural rocks and the grain size or permeability of such materials. We have also presented a simple theoretical analysis of the results. Many other potential applications of the methods are conceivable, both for natural rocks and for media other than natural rocks. Both the experiments and the theoretical interpretations presented here are relatively simple: further refinements of both are necessary to provide a detailed quantitative understanding. For example, the interpretation of experiments is complicated by pore-filling and pore-lining substances such as clay. Another complication, not discussed here, is the effect of topology.[27] In measurements such as described here, in which the contrast between the indices of refraction of grain and pore fluid is not too great, light is transmitted through both media and the influence of pore topology on light transmission is probably not critical. In cases of greater contrast, this topology may be more important, possibly leading to an even stronger correlation between optical transmission and fluid permeability. Finally, we note that light of different wavelengths may elicit other types of information, especially if the relevant indices of refraction are frequency dependent.

## ACKNOWLEDGMENTS

This work was supported in part through NSF Grant Nos. DMR 87-18874 and DMR 90-20994, and by the Ohio Supercomputer Center. We thank Dr. F. G. McCaffery for helpful discussions.

## APPENDIX: CALCULATION OF $l_{\mathrm{el}}$ FOR A RANDOM COMPOSITE IN THE SHORT-WAVELENGTH LIMIT

We want to compute an elastic mean free path for light scattering from a random composite in the short-wavelength limit. Thus, we imagine a volume $V$ of random composite, embedded in a homogeneous medium of dielectric constant $\epsilon_0$ (which may be a function of frequency). Writing the dielectric function at point $\mathbf{r}$ as $\epsilon(\mathbf{r})=\epsilon_0(\mathbf{r})+\delta\epsilon(\mathbf{r})$, we have a linear relation between $\mathbf{D}(\mathbf{r})$ and $\mathbf{E}(\mathbf{r})$ (suppressing the frequency dependence):

$$\mathbf{D}(\mathbf{r})=\epsilon_0\mathbf{E}(\mathbf{r})+\delta\epsilon(\mathbf{r})\mathbf{E}(\mathbf{r}) \; . \tag{A1}$$

We now assume that the composite is subject to an incident plane wave with electric field

$$\mathbf{E}_0(\mathbf{r},t)=\mathbf{E}_0\exp(i\mathbf{k}_0\cdot\mathbf{r}-i\omega t) \; , \tag{A2}$$

where $k_0=\omega\sqrt{\epsilon_0}/c$. If there were a homogeneous medium of dielectric constant $\epsilon_0$ filling all space, the electric displacement would be simply $\mathbf{D}_0=\epsilon_0\mathbf{E}_0$. Because of the presence of the composite, the total displacement is $\mathbf{D}=\mathbf{D}_0+\mathbf{D}_s$, where $\mathbf{D}_s$ is an additional scattering term. In the Born approximation, and at distances far from the composite in comparison to its linear dimensions, it can be shown from Maxwell's equations that

$$\mathbf{D}_s(\mathbf{r})=\frac{e^{ikr}}{r}\mathbf{f}(\hat{\mathbf{e}},\hat{\mathbf{e}}_0) \; , \tag{A3}$$

where $\mathbf{k}$ is the scattered wave vector, $k=\omega\sqrt{\epsilon_0}/c$ (elastic scattering), and $\hat{\mathbf{e}}$ and $\hat{\mathbf{e}}_0$ are unit polarization vectors parallel to the electric field vectors of the scattered and incident waves, respectively. In the Born approximation, the scattering amplitude $\mathbf{f}(\hat{\mathbf{e}},\hat{\mathbf{e}}_0)$ takes the form

$$\mathbf{f}(\hat{\mathbf{e}},\hat{\mathbf{e}}_0)=-\frac{1}{4\pi}\mathbf{k}\times\mathbf{k}\times\int\frac{\delta\epsilon(\mathbf{r}')}{\epsilon_0}\mathbf{D}_0(\mathbf{r}')e^{-i\mathbf{k}\cdot\mathbf{r}'}d^3r' \; . \tag{A4}$$

The corresponding differential cross section is

$$\frac{d\sigma}{d\Omega}=\frac{\langle|\mathbf{f}(\hat{\mathbf{e}},\hat{\mathbf{e}}_0)|^2\rangle}{|\mathbf{D}_0|^2} \; . \tag{A5}$$

where $\langle\cdots\rangle$ denotes an ensemble average over the configurations of the random function $\delta\epsilon(\mathbf{r}')$. Substituting Eq. (A4) into Eq. (A5), and averaging over polarizations of the incident radiation, one obtains

$$\frac{d\sigma}{d\Omega}=\frac{k^4}{32\pi^2\epsilon_0^2}(1+\cos^2\theta)\int\langle\delta\epsilon(\mathbf{r}')\delta\epsilon(\mathbf{r}'')\rangle e^{-i\mathbf{q}\cdot(\mathbf{r}'-\mathbf{r}'')}d^3r'd^3r'' \; . \tag{A6}$$

where $\mathbf{q}=\mathbf{k}-\mathbf{k}_0$, $\theta$ is the angle between $\mathbf{k}$ and $\mathbf{k}_0$, and the integral runs over the volume $V$ of the composite.

To calculate the differential scattering cross section, one must know the form of the correlation function $\langle\delta\epsilon(\mathbf{r}')\delta\epsilon(\mathbf{r}'')\rangle$. If one assumes an exponential correlation function of the form

$$\langle\delta\epsilon(\mathbf{r})\delta\epsilon(\mathbf{r}')\rangle\approx\langle(\delta\epsilon)^2\rangle\exp\left[\frac{-|\mathbf{r}-\mathbf{r}'|}{\xi}\right] \; , \tag{A7}$$

where $\xi$ is an appropriate correlation length (assumed to be much smaller than the dimensions of the composite), one obtains

$$\frac{d\sigma}{d\Omega}=\frac{Vk^4\langle(\delta\epsilon)^2\rangle}{4\pi\epsilon_0^2}\,\frac{\xi^3(1+\cos^2\theta)}{[1+2k^2\xi^2(1-\cos\theta)]^2} \; . \tag{A8}$$

The elastic mean free path is the distance traveled by a photon before it loses memory of its original direction. By analogy with the corresponding calculation in the theory of electronic mean free paths,[28] this is obtained by weighting the differential-scattering cross section by a factor $(1-\cos\theta)$, which favors large angles. We then find that the mean free path $l_{\mathrm{el}}$ is given by

$$\frac{1}{l_{\mathrm{el}}}\equiv\frac{1}{V}\int\frac{d\sigma}{d\Omega}(1-\cos\theta)d\Omega \tag{A9}$$

$$=\frac{k^4\langle(\delta\epsilon)^2\rangle}{2\epsilon_0^2}\xi^3 I \; , \tag{A10}$$

where

$$I=\left[\frac{3+8k^2\xi^2+8k^4\xi^4}{16k^8\xi^8}\right]\ln(1+4k^2\xi^2)-\frac{(3+14k^2\xi^2+16k^4\xi^4)}{4k^6\xi^6(1+4k^2\xi^2)} \; . \tag{A11}$$

In the long-wavelength limit ($k^2\xi^2\ll 1$), $I=\frac{8}{3}$ and $1/l_{\mathrm{el}}$ is proportional to $k^4$, as expected for Rayleigh scattering. In the short-wavelength limit ($k^2\xi^2\gg 1$), we find

$$\frac{1}{l_{\mathrm{el}}}=\frac{\langle(\delta\epsilon)^2\rangle}{4\epsilon_0^2}\,\frac{\ln(2k^2\xi^2)}{\xi} \; , \tag{A12}$$

with is equivalent to Eq. (3).

---

[1] A. I. Levorsen, *Geology of Petroleum* (Freeman, San Francisco, 1967).

[2] J. Bear, *Dynamics of Fluids in Porous Media* (American Elsevier, New York, 1972).

[3] R. E. Collins, *Fluid Flow Through Porous Materials* (Reinhold, New York, 1961).

[4] A. E. Scheidegger, *The Physics of Flow Through Porous Media* (University of Toronto Press, Toronto, 1974).

[5] F. A. L. Dullien, *Porous Media: Fluid Transport and Pore Structure* (Academic, New York, 1979).

[6] Y. Bernabé, in *Fault Mechanics and Transport Properties of Rocks: The Brace Volume,* edited by T. F. Wong and B. Evans (Academic, New York, in press).

[7] B. F. Swanson, J. Pet. Technol. **33**, 2498 (1981).

[8] A. J. Katz and A. J. Thompson, Phys. Rev. B **34**, 8179 (1986).

[9] M. A. Chandler, D. J. Goggin, and L. W. Lake, J. Sediment Petrol. **59**, 613 (1989).

[10] A. E. Scheidegger, Geofis. Pura Appl. **28**, 75 (1956).

[11] F. M. Auzerais, D. V. Ellis, S. M. Luthi, E. B. Dussan, and B. J. Pinoteau (unpublished).

[12] K. M. Yoo, Feng Liu, and R. R. Alfano, Phys. Rev. Lett. **64**, 2647 (1990).

[13] L. F. Gate, J. Phys. D **4**, 1049 (1971).

[14] A. Ishimaru, Y. Kuga, R. L. T. Cheung, and K. Shimizu, J.

Opt. Soc. Am. **73**, 131 (1983).

[15] A. Ishimaru and Y. Kuga, J. Opt. Soc. Am. **72**, 1317 (1982).

[16] A. Z. Genack, Phys. Rev. Lett. **58**, 2043 (1987).

[17] D. J. Pine, D. A. Weitz, P. M. Chaikin, and E. Herbolzheimer, Phys. Rev. Lett. **60**, 1134 (1988).

[18] M. P. Van Albada, J. F. de Boer, and A. Lagendijk, Phys. Rev. Lett. **64**, 2787 (1990).

[19] S. Feng, L. Golubovic, and Y. C. Zhang, Phys. Rev. Lett. **65**, 1028 (1990).

[20] W. A. Deer, R. A. Howie, and J. Zussman, *Rock-forming Minerals* (Wiley, New York, 1963), Vol. 4.

[21] A. Ishimaru, *Wave Propagation and Scattering in Random Media* (Academic, New York, 1978), Vol. 2.

[22] *Handbook of Chemistry and Physics,* 53rd ed., edited by R. C. Weast (Chemical Rubber Co., Cleveland, 1972), pp. E-208 and E-209. Crystalline quartz is birefringent, with principal indices of refraction 1.55 and 1.54 in the visible. We have arbitrarily assumed isotropy with $n = 1.55$ in our modeling.

[23] J. D. Jackson, *Classical Electrodynamics* (Wiley, New York, 1975), Chap. 7.

[24] R. Jullien and R. Botet, J. Phys. (Paris) **50**, 1983 (1989) have used a procedure similar to ours to compute the scattering cross section of fractal aggregates, in the limit when the particles making up the aggregates are large compared to the wavelength. The Monte Carlo criterion used by these authors for following the reflected or refracted wave is slightly different from ours but should lead to the same weighting of transmitted and reflected waves in the limit of a sufficiently large number of incident rays.

[25] Thus, we do *not* assume that the transmitted intensity falls off exponentially with thickness. In fact, even for a perfectly nonabsorbing medium in the diffusion limit, the transmission does not fall off exponentially. See, e.g., P. W. Anderson, Philos. Mag. B **52**, 505 (1985); D. J. Durian, D. A. Weitz, and D. J. Pine, Science **252**, 686 (1991); or Ishimaru, *Wave Propagation and Scattering in Random Media* (Ref. 21).

[26] For a sufficiently thick sample, the width of pulses such as shown in Fig. 4 is determined by the diffusion coefficient for light, $D = v_E l_{\rm el}/3$, where $v_E$ is a suitable velocity of energy transport [see M. P. Van Albada, B. A. Van Tiggelen, A. Lagendijk, and A. Tip, Phys. Rev. Lett. **66**, 3132 (1991)]. Such pulse profiles have been calculated by a number of authors by solving the diffusion equation. The tails of these distributions can be analyzed to give the absorption coefficient of the medium. See, for example, G. H. Watson, P. A. Fleury, and S. L. McCall, Phys. Rev. Lett. **58**, 945 (1987).

[27] A. H. Thompson, A. J. Katz, and C. E. Krohn, Adv. Phys. **36**, 625 (1987).

[28] See, for example, J. M. Ziman, *Principles of the Theory of Solids* (Cambridge University Press, Cambridge, 1964), pp. 187f.

View publication stats